Multi-objective optimization of AAJM process parameters for cutting of B$_4$C/Gr particles reinforced Al 7075 composites using RSM-TOPSIS approach

Murahari Kolli[1] · A. V. S Ram Prasad[2] · Dasari Sai Naresh[3]

Abstract

Abstract The present study deals with the machining of hybrid Al 7075/B$_4$C/Gr composite using Abrasive Aqua Jet Machining. The effects of selected input factors, i.e., water jet pressure (WJP), stand-off distance (SOD), and traverse speed (TS) on the performance characteristics, namely taper angle (TA), surface roughness (Ra), and the material removal rate (MRR) are investigated. The experimental runs and test strategies are formulated using the Response Surface Methodology-Central Composite Design approach. Analysis of Variance (ANOVA) was used to examine the effect of input factors and their interactions with performance characteristics. MRR, Ra, and TA optimum condition and mathematical equations were also developed. Further, the multi-optimization method "Technique for Order of Preference by Similarity to Ideal Solution" is considered to find out the best combinations of input factors for optimized output factors on the hybrid composite. The ANOVA results confirm that among the input factors, WJP and SOD are the most significant factors, and the percentage distribution of input factors are found to be jet pressure (55.21%), stand-off distance (23.36%), and traverse speed (2.56%). The multi-objective optimum conditions of the input factors are WJP (A$_1$) 210 bar, SOD (B$_1$), and TS (C$_3$) 30 mm/min, that produce optimal values of the considered responses, i.e., MRR up to 4.8703 mm^3/min, Ra up to 3.57 μm and TA up to 0.189°. The TA has improved by 49.6% through the multi-objective optimum results when compared with single parameter optimized results.

Article Highlights

- Hybrid Al7075/B$_4$C/Gr composite fabricated through the rotary stir casting technique
- Experimental planning and designing layouts using Response Surface Methodology scheme and mathematical equations are produced with Design Expert 11.0.
- The best TA was obtained by RSM-TOPSIS approach, found at a lower WJP and SOD and a higher TS.

✉ Murahari Kolli, kmhari.nitw@gmail.com | ¹Department of Mechanical Engineering, Lakireddy Bali Reddy College of Engineering, Mylavaram, Krishna District, Andhra Pradesh 521230, India. ²Department of Mechanical Engineering, Koneru Lakshmaiah Education Foundation, Vaddeswaram, Guntur, Andhra Pradesh 521503, India. ³R&D Mechatronics, Design and Engineering, VEM Technologies Pvt Ltd, Hyderabad, Telangana 502321, India.

1 Introduction

A significant challenge in the development of materials with high strength to weight ratio in material sciences and engineering remains even today. Following the fast-paced development of science and technology, aluminium and its alloys have become a pertinent area of constant research, consistently improvising and imparting practical applications due to their low density, high strength, and high ductility. Al composite/hybrid composites are fabricated through mixing of two or more materials that chemically and physically exist in distinct phases. Al_2O_3, SiC, B_4C, Mg_2, Si, TiC, etc. reinforcement particles are added to the base materials to enhance their properties. Hybrid metal matrix composites (HMMCs) can be sorted into a type of reinforced metal matrix composites and are also extensively used as composite materials [1, 2]. HMMC's constitute an important member of a group of structural materials that find widespread applications in automotive, defense, and aerospace due to low density, high specific strength and modulus, excellent wear resistance, higher service temperature, and comparatively higher physical and mechanical properties than monolithic and composite materials[3].

However, machining of HMMCs is a very challenging task in the present scenario because of the hard, reinforced, abrasive particles present in their matrix. They pose significant difficulties in machining through traditional machining processes [4]. Milling, drilling, shaping, turning, and sawing are some of the conventional machining methods used for machining of HMMCs. But, none of the conventional machining methods, when used to machine HMMC's, can yield high dimensional accuracies and can become very expensive to produce such results. Apart from these reasons, defects like cracks and voids on the machined surface of HMMC are commonly found in samples machined through conventional routes. [5, 6]. The replacement for machining HMMCs with unconventional machining methods such as laser beam machining, plasma machining, water jet machining, electrical discharge machining, wire electrical discharge machining, etc. is being widely explored [7].

AAJM is one such adaptable and accepted nontraditional machining process for cutting, trimming, drilling, and deburring hard and brittle materials like ceramics, composites, and HMMC. AAJM is highly advantageous compared to conventional machining due to a high degree of machining flexibility, low machining forces, and less heat-affected zone (HAZ). Another advantage of AAJM is that the cutting cost is nominal compared to other conventional machining processes.

Thamizhvalavan et al. studied the machinability characteristics of Abrasive Aqua Jet (AAJ) on Al 6063/ B_4C/ $ZrSiO_4$ composites with 5% of fixed reinforcement particles added to the matrix material. The results testified that maximum MRR and minimum Ra and kerf TA were obtained at the higher abrasive flow rate, aqua WJP and lower TS [8]. Manoj et al. considered the TiB_2 reinforcement particles as reinforcements into Al 7075 matrix and fabricated the Al 7075/TiB_2 composite for AWJ machining. WJP, TS and SOD have been selected as machining factors to estimate the response factors like TA, MRR and Ra by adopting the Taguchi-DEAR approach. They found that the significance of WJP was greater than other factors on TA, MRR and Ra of AWJ machining [9].

Dhanawade et al. investigated the effect of AWJM on carbon epoxy composite. RSM approach was used to develop a mathematical model and to find out the significance of control factors to influence the responses. It concluded that the fitted mathematical model for Ra is in good agreement with the experimental result [10]. Siddiqui and Shukla applied a combined approach by Taguchi-PCA to evaluate the performance measures of AAJM with multiple quality characteristics [11]. Sasikumar et al. optimized the AAJM parameters on Al 7075/TiC/B_4C using RSM-Box Behnken Design (BBD) approach. The performance parameters of study considered are Ra, kerf top and kerf bottom against the AAJM input factors, namely SOD, TS and WJP. The results confirmed that the most significant contributing factors are TS and WJP respectively and also regression models for kerf characteristics are developed [12]. Kumar et al. examined the titanium-carbon fiber-reinforced plastics-titanium hybrid laminate materials using AWJM with TS, WJP, and SOD as input parameters. They employed the RSM-CCD approach to analyze the influence factors on quality characteristics of MRR and Ra. It has been observed that WJP and TS had maximum influence on the MRR and Ra [13].

Iqbal et al. considered the factorial experimental layout to examine the AAJM process factor's influence on performance characteristics like % of striation free surface, cutting width, the surface texture of Al 2219 and AISI 4340 [14]. Kumar et al. investigated the parametric effect of AWJM on Ra of Inconel 718 alloy using a combined RSM-BBD approach and successfully formulated quadratic models of Ra in terms of WJP, SOD. The results established an excellent interrelationship between experimental and predicted values at 95% confidence level. They concluded that TS and abrasive flow rate substantially affected the Ra. WJP was insignificant in their studies but WJP's interactions were reported to be highly significant [15]. Ravi Kumar et al. studied the AAJM factors on Al/WC composite using the RSM-CCD approach. In their process, the input factors like SOD, TS and percentage of TiC were considered. They confirmed that MRR was

most affected by the TS followed by the percentage of TiC and SOD respectively: at the same time, Ra was highly influenced by the percentage of TiC, followed by TS and SOD [16].

Furthermore, a little to scarce amount of scientific studies were carried out on hybrid optimization techniques of various processes. Tofigh et al. studied compocast process parameters optimization of nano A356/Al2O3 composite with neuro-fuzzy inference system and particle swarm optimization. They have also carried out investigations on the abrasive wear behavior of Al/B_4C composite with a pin-on-disc machine using hybrid particle swarm optimization-artificial neural network (PSO–ANN) technique. The results confirmed that the novel search technique has eliminated premature convergence problems that are common with high dimensional problems [17, 18]. Shabani et al. optimized the process parameters of pressure-assisted semi-solid processing of A360/TiC nano composite using the ANFIS-PSO technique. It was noted that the trained model could behave erratically in unseen input conditions and was not easy to interpret in case of inadequate training dataset; since, in such hybrid models the learning was entirely data-driven with stringent requirements on the quality of the training dataset [19].

Akbari et al. examined the microstructural and mechanical properties of A356/B_4C composites using FSP. The FSP parameters optimization was selected as an artificial neural network (ANN) and non-dominated sorting genetic algorithm-II (NSGA-II). The results confirmed that a strong relationship was established between the FSP parameters and microstructural and mechanical properties of the composites [20]. Shabani et al. implemented the ANFIS-PSO algorithm to predict the experimental results and optimize the processing parameters of Al/Al2O3 composites and Al composite. ANFIS-PSO algorithm considered for the casting process had resulted in enhancement of the results [21]. Shamsipour et al. evaluated the wear behavior of optimized parameters of Al/TiC nanocomposite using ANFIS and PSO techniques [22].

The literature survey indicates that some research work was published on the machining of Al 7075 composite with the AAJM process [8, 9]. Furthermore, very scarce or no research has been carried out on Al 7075/B_4C/Gr with the RSM-CCD approach. The present work investigates the effect of with process parameters of AAJM on hybrid Al 7075/B_4C/Gr composite. The main objective of the study is the multiparametric optimization of AAJM process parameters using the RSM-CCD-TOPSIS approach. WJP, SOD, TS are selected as AAJM process input factors. The AAJM output parameters

like TA, Ra and MRR are investigated. The importance of the AAJM input parameters on machining output characteristics was examined by TOPSIS. TOPSIS is one of the multi-criteria decision-makers. It is based on the criteria weights that are assigned by the support on the information and numerical data, to determine the rating of alternatives and for evaluation, prioritization, and selection. This technique compares a set of experimental conditions on predetermined performance characteristics. The best input factors and their percentage values were found out using the ANOVA tests. Furthermore, a mathematical relationship between the measured performance characteristics and the AAJM process input factors is formulated. Finally, using the multi-objective approach of TOPSIS has been carried out within the tested range of AAJM parameters.

2 Experimental procedure

2.1 Material fabrication

The Al 7075 alloy is considered as the parent material. The elemental composition of Al 7075 alloy is presented in Table 1. In the current investigation, B_4C and Gr are used as reinforcement particles. B_4C and Gr reinforcement particle sizes are below 25–30 μm as depicted in Figs. 1 and 2 respectively. The preparation of hybrid composite material was done by mixing B_4C and Gr particles with parent metal, and the B_4C incrementally varying at 4% by weight
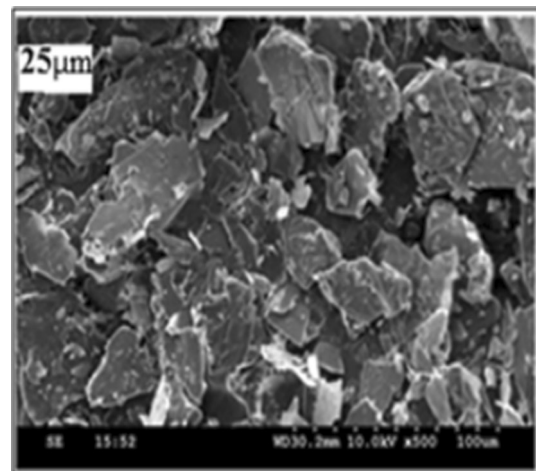
Fig. 1 SEM image of graphite powder (Gr) particles

Table 1 Chemical composition of Al 7075 alloy

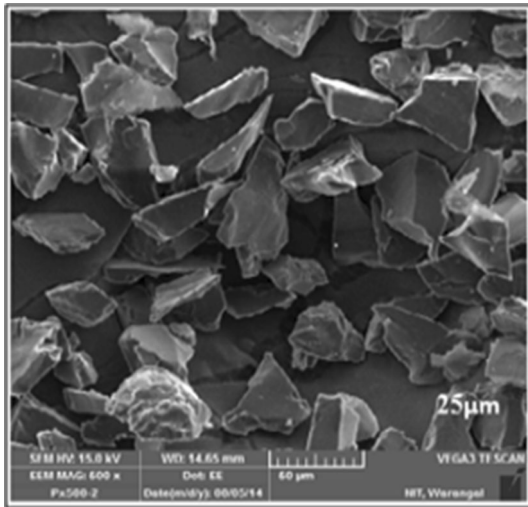| Elements	Zn	Mg	Cu	Si	Mn	Fe	Cr	Ti	Al
Wt%	5.56	2.71	1.42	0.33	0.21	0.34	0.27	0.12	Remaining

Fig.2 SEM image of boron carbide (B_4C) powder particles

Fig.3 Stir casting machine for fabrication of composite

and Gr particles being kept constant at 3% by weight in the matrix. The rotary stir casting technique is used to fabricate the HMMCs, as depicted in Fig. 3. The fabricated HMMCs chemical composition is mentioned in Table.2.

2.2 Machine tool

The experiments are conducted on an Abrasive Aqua Jet Machine of MJ TT model with a CNC controller (Make: Citizen, India). The input factors like WJP, SOD and TS are considered and maintained at equal levels as mentioned in Table 3. During the entire cutting process, the machining parameters of AAJM such as orifice diameter, impact angle and nozzle diameter are kept unchanged. All AAJM

Table 3 Levels of input factors

Input factors	Units	Level 1	Level 2	Level 3
		− 1	0	+1
Water jet pressure(WJP)	Bar: (A)	210	225	240
Standard of Distance(SOD)	mm: (B)	2	2.5	3.0
Traverse speed (TS)	mm/min: (C)	10	20	30

machined samples are cut as a square hole of $15 \times 15 \times 10$ mm dimension as shown in Fig. 4.

2.3 Performance evaluation

For this study, the cutting performance evaluations are considered based on the output measurements like TA, Ra and MRR. The TA is measured for taperness of the AAJM machined composite surface, as it is a significant output measurement and is necessary to have a minimum kerf taper maintained during the cutting by AAJM to maintain dimensional stability. The TA is measured (top and bottom) using the Coordinate Measuring Machine (CMM). Ra is measured by using handy surf equipment at various locations on machined samples (Make: Zeiss, India, Model: E-35B). To calculate the MRR by weight, differences of the before and after machined-sample of the composite are measured by an electronic digital weighing machine (Make: Citizen, India, Model: CY 204) with least count of 0.0001 g.

2.4 Design of experiments (DOE)

The experiments are designed using RSM-CCD plan to arrive at the best optimal AAJM parameters for Al7075/B_4C/Gr composite.

2.4.1 RSM for single objective optimization

RSM as a subcategory of design of experiments (DOE) technique widely used in the planning, design, and optimization of the manufacturing processes. It is a statistical tool that is highly capable of analyzing and optimizing the problem [23]. One of the essential statistical RSM-CCD techniques is used for the present investigation, which has the accompanying points of interest: CCD approach isn't just compelling in foreseeing the reaction of the fitted

Table 2 Chemical composition of hybrid Al 7075/B_4C/Gr alloy

Elements	Zn	Mg	Cu	Si	Mn	Fe	Cr	Ti	Al
Wt%	5.34	2.12	1.49	0.49	0.02	0.2	0.19	0.03	Remaining

Fig.4 AAJ machining setup

model along with a minimal measure of investigations. It assists in the investigation of the collaborations between various factors as well. Besides, it can assess the elements of the quadratic model productively and maintain a strategic difference from treatment mixes at an extreme range. The fundamental reason for the adoption of this approach is to investigate the connection between the input parameters and the output measurements on the hybrid Al 7075/B_4C/Gr composite machining.

In the CCD technique, for the construction of a second-order polynomial model, as given by Eq. (1), each factor is varied at three levels (+, 0, -). The specific advantage of this technique is that it is not necessary to run experiments in all combinations of factors when the number of factors becomes three. The design can be executed using a fraction of the total number of variable combinations. The possible design options can be either regular fractional or minimum run experimental resolution. It has a smooth function that enhances the best performance characteristics of a particular study and hence, it eliminates the unwanted parameters/factors. It reduces the effect of noise and allows for the use of derivative-based algorithms [24, 25].

$$Z = b_0 + \sum_{n=1}^{n} \left(b_i Y_i \right) + \sum_{i=1}^{n} \left(b_{ii} Y_i^2 \right) + \sum_{i=1}^{n-1} \sum_{j=1}^{n} \left(b_{ij} Y_i Y \right) \qquad (1)$$

The RSM models are developed for the sustainable measures of optimum response values using Design Expert® 11.0 (DOE) statistical software. The aim is to identify the best response values and these are influenced by variable dependent factors from the DOE. Three input factors and three levels are selected with the RSM-CCD layout. The input factors are WJP, SOD and TS. The number of input factors and their values can be observed in Table 3. For the AAJM process, TA and Ra are "the lower the better" characteristics and MRR is the "higher the better" performance characteristic.

In general, the results of single measured characteristics can be compensated by any one of the performance measured characteristics in the AAJM cutting process. For that cause, the best condition of the multi-performance measures is tougher than the single performance measures. In the present work, an attempt was made to investigate the best multiple degree characteristics of the AAJM process from the RSM-CCD plan through the TOPSIS approach.

2.4.2 TOPSIS for multi-objective optimization

In 1995, Hwang and Yoon initially developed the TOPSIS technique to evaluate the preference for an order using similarity for an ideal solution. A theoretical solution to the problem is seen as an ideal solution when the values of all attributes correspond to the minimum values of the attributes. TOPSIS targets to get the best minimum and maximum way of the distance from the positive solution and negative solution (hypothetically best and hypothetically worst) arranged and subsequently the development of the preorder through similitude with the perfect arrangement.

The following steps are involved in the TOPSIS approach [26, 27].

Step 1: Evaluate the RSM-CCD experiments through the performance measurements, namely TA, Ra and MRR.

Step 2: Design a decision matrix as shown below, which consists of 'm' alternatives and 'n' attributes.

Step 3: Calculate the normalized decision matrix of each response measurement using Eq. (2)

$$r_{ij} = \frac{x_{ij}}{\sqrt{\sum_{i=1}^{m} x_{ij}^2}} \; j = 1, 2, \ldots, n \qquad (2)$$

where

x_{ij} represents the actual value of ith value for j^{th} experimental run.

Step 4: Find out the weighted normalized decision matrix considering Eq. 3.

$$V_{ij} = W_j \times r_{ij} \quad (3)$$

where

r_{ij} is a normalized decision matrix.

W_j has associated weights for matrix.

V_{ij} is constructed weighted normalized decision matrix.

By using equation number (3) i.e., multiplying the normalized decision matrix with its associated weights, the weighted normalized decision matrix is further developed [28, 29]. The standard deviation approach is applied for the present study, to find the unbiased weight of individual measurements. Based on the TOPSIS approach the significant task is to find the distribution of weights. Ram Prasad et al. adopted a measurement level of standardization to calculate weights with help of the standard deviation method [30].

Step 5: The subsequent step is to find out the best (positive V_j^+) and worst (negative V_j^-) solutions with the help of the following Eqs. 4 and 5.

$$V_j^+ = \left\{ \overset{max}{\underset{i=1}{\sum}} V_{ij} / j \in J, \overset{min}{\underset{i=1}{\sum}} V_{ij} / j \in J^l \right\} \quad (4)$$

$$V_j^- = \left\{ \overset{min}{\underset{i=1}{\sum}} V_{ij} / j \in J, \overset{max}{\underset{i=1}{\sum}} V_{ij} / j \in J^l \right\} \quad (5)$$

Step 6: The next step is to work out the separation of individual alternatives from the best ideal S_i^+ solution and worst ideal S_i^- solution using the following Eqs. 6 and 7.

$$S_i^+ = \sqrt{\sum_{j=1}^{n} \left(V_{ij} - V_j^+ \right)^2}, \ i = 1, 2, \ldots, m \quad (6)$$

$$S_i^- = \sqrt{\sum_{j=1}^{n} \left(V_{ij} - V_j^- \right)^2}, \ i = 1, 2, \ldots, m \quad (7)$$

Step 7: The Final step is the calculation of closeness coefficient (C_i^+) for individual performance measures adopting the following Eq. 8.

$$C_i^+ = \left(\frac{S_i^-}{(S_i^+ + S_i^-)} \right) \quad (8)$$

3 Results and discussion

This section can be divided into three parts. The first part deals with single performance characteristics optimization (3.1), and the second part discusses multiple objective parameters optimization using the TOPSIS approach (3.2) and the final part verifies and discusses the conformation

Table 4 RSM-CCD layout and their experimental values

Run Order	Pressure (A)	Stranded of Distance(B)	Traverse speed (C)	MRR (mm^3/min)	Ra (µm)	Taper angle(0°)
1	225	3	20	4.7546	3.77	0.854
2	225	2.5	10	3.8494	3.08	0.691
3	240	2.5	20	3.8799	4.19	0.754
4	210	2	10	4.4927	2.65	0.357
5	210	3	10	5.3118	2.91	0.543
6	240	3	10	4.2640	4.26	0.897
7	225	2.5	20	4.0951	3.43	0.658
8	225	2.5	20	4.0176	3.39	0.697
9	240	3	30	4.9692	4.62	1.041
10	225	2.5	20	4.1239	3.46	0.667
11	225	2.5	20	4.1645	3.48	0.653
12	225	2.5	20	4.0464	3.44	0.692
13	225	2.5	20	4.1439	3.47	0.695
14	225	2	20	4.4317	3.24	0.655
15	210	2	30	4.6703	3.74	0.194
16	210	2.5	20	4.3510	3.37	0.375
17	225	2.5	30	4.3771	3.93	0.746
18	240	2	10	3.3010	3.84	0.447
19	240	2	30	4.7613	4.22	0.802
20	210	3	30	4.9310	3.95	0.483

experiments of Al 7075/B$_4$C/Gr composite material (3.3). The RSM-CCD experimental layout and their results are presented in Table 4.

3.1 Single performance characteristics optimization

3.1.1 Effect of parameters on material removal rate (MRR)

The ANOVA result for MRR is as shown in Table 5. The compliance of P-value less than 0.05 levels i.e., at 95% significance reveals a significant model. The model F-value at 183.37 endorses that the model is exceptionally significant. The "Lack of Fit" F-Value standing at 1.20 is evidence that the lack of fit is insignificant. The Lack of Fit F-Value has a chance of occurrence due to noise at 43.9%. The R^2 value and Adj. R^2 are in great agreement with 98.83% and 98.29% respectively. From Table 5 it can be inferred that the F-values of A, B, C and interactions AC and BC are quite significant and influence the MRR to a great extent.

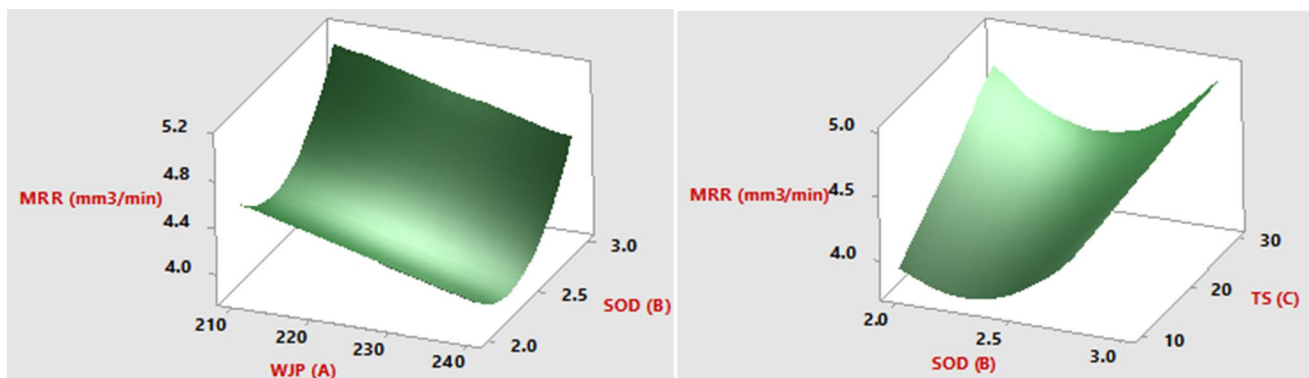The mathematical model for the MRR is Eq. 9.

The 3D graphs of MRR for the significant interaction between input factors, namely WJP, SOD and TS are shown in Fig. 5a and b, respectively. It testifies that MRR approaches its maxima at the higher levels of SOD, TS and to its minima at WJP. The MRR was observed to be diminishing with the WJP. However, it should be noted that the proper interaction of WJP and TS are necessary to make a significant effect on MRR [31].

In the present investigation, due to proper interactions between WJP and TS, low levels of WJP were sufficient to induce the impact and kinetic energy that is passed on to the target point of the work-piece material that resulted in B$_4$C and Gr particles being easily pulled out of the composite material. Similar type of results were obtained in the studies led by some of the coauthors, they reported improved cutting by enhancing the water WJP. In the same way it was observed that MRR increases with increasing the value of SOD. This may be due to the high impact energy of the abrasive on the hybrid composite material which results in an ineffective cut of the MMC

$$MRR = 25.530 - 0.05669 * A - 8.506 * B - 0.3371 * C + 1.935 * B * B + 0.001974 * A * C - 0.03284 * B * C \qquad (9)$$

Table 5 ANOVA for MRR of Al/B$_4$C/Gr composite material	SS	DF	Seq SS	Adj SS	MS	F-Value	P-Value
	Model	6	4.03630	4.03630	0.67272	183.37	0.000
	Linear	3	1.94872	1.94872	0.64957	177.06	0.000
	A	1	0.66641	0.66641	0.66641	181.65	0.000
	B	1	0.66232	0.66232	0.66232	180.53	0.000
	C	1	0.61998	0.61998	0.61998	168.99	0.000
	2-Way Interaction	2	0.91694	0.91694	0.45847	124.97	0.000
	A*C	1	0.70130	0.70130	0.70130	191.16	0.000
	B*C	1	0.21564	0.21564	0.21564	58.78	0.000
	Error	13	0.04769	0.04769	0.00367		
	Lack of fit	8	0.03136	0.03136	0.00392	1.20	0.439
	Pure Error	5	0.01633	0.01633	0.00327		
	Total	19	4.08399				

Fig.5 Response plot for MRR (mm³/min)

and enhances the MRR Enhancement in TS directly influences the MRR of the hybrid composite [31, 32]. At the same time, as hard reinforcement particles were eroded rapidly or pushed out at higher TS led to the achievement of maximum MRR [33]. The optimum condition of MRR is obtained at the $A_1B_3C_1$. It has been confirmed that lower values of WJP (210 bar), higher values of SOD (3 mm), and lower values of TS (10 mm/min) gives the maximum MRR value at 5.3155 mm³/min. On the other hand, the combi-

significance notifies that the model is a significant model. The model F-value at 231.57 validates that the model is exceptionally significant. F-value standing at 4.52 of 'Lack of Fit' confirms its insignificance. Furthermore, the lack of fit may occur at a 5.7% probability due to noise. R^2 and Adj. R^2 are complimentary at 99.07% and 98.65% respectively. The ANOVA Table 6 suggests that WJP and TS have been major factors to control the Ra.

The mathematical model for Ra is formulated Eq. 10.

$$Ra = 62.45 - 0.5770 * A - 0.987 * B + 0.2960 * C + 0.001367 * A * A + 0.00600 * A * B - 0.001150 * A * C \tag{10}$$

nation of WJP and TS has proven to be most significant in determining the MRR.

3.1.2 Effect of parameters on surface roughness (Ra)

ANOVA results for Ra are presented in Table 6. The agreement of P-value at less than 0.05 levels, i.e., at 95%

The 3D response plots of Ra with the best interaction input parameters, WJP and SOD, WJP and TS are depicted in Figs. 6a and b respectively. Ra is directly proportional to WJP, SOD and TS. Normally, higher WJP caters more energy to the surface of the composite which influences the desired contact area that leads to the formation of more voids [34]. Whenever the WJP offers suitably high energy to reinforcement particles, the machining process is acceptable to be passed out without

Table 6 ANOVA for Ra of Al/B₄C/Gr composite material

| SS	DF	Seq SS	Adj SS	MS	F-Value	P-Value
Model	6	4.46902	4.46902	0.74484	231.57	0.000
Linear	3	3.74198	3.74199	1.24733	387.79	0.000
A	1	2.02500	2.02500	2.02500	629.57	0.000
B	1	0.32942	0.32942	0.32942	102.42	0.000
C	1	1.38756	1.38756	1.38756	431.39	0.000
2-Way Interaction	2	0.25425	0.25425	0.12713	39.52	0.000
A*B	1	0.01620	0.01620	0.01620	5.04	0.043
A*C	1	0.23805	0.23805	0.23805	74.01	0.000
Error	13	0.04181	0.04181	0.00322		
Lack of fit	8	0.03673	0.03673	0.00459	4.52	0.057
Pure Error	5	0.00508	0.00508	0.00102		
Total	19	4.51083				
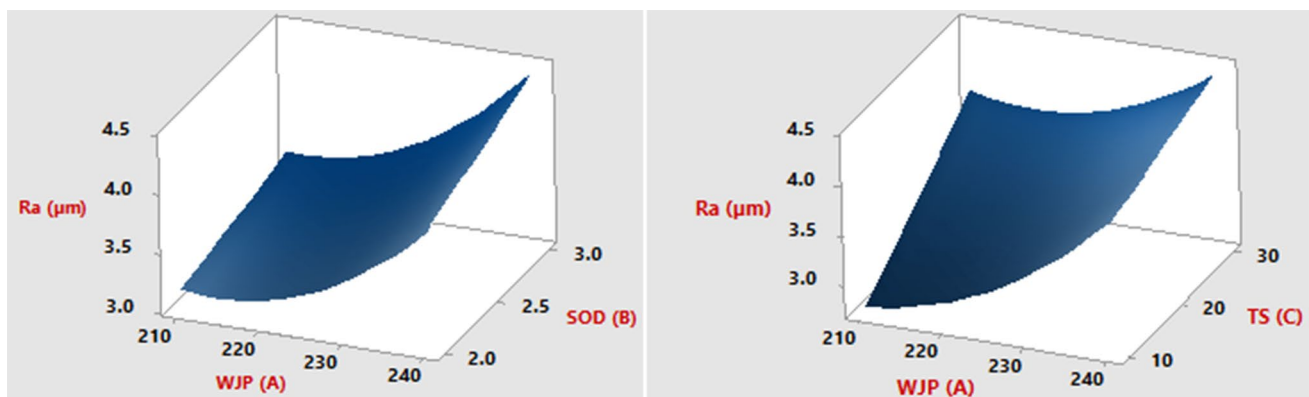
Fig.6 Response plot for Ra (μm)

stern jet flirtation which will indicate the less waviness pattern on the surface [35]. Similarly, the higher Ra is obtained for higher SOD because of the higher external drag from the surroundings of the target. The enhancement in SOD makes the jet to enlarge before hitting the target material, thus reducing the kinetic energy of the jet. Related to another factor, Ra increased with TS; higher TS will hinder the total process of the kerf wall. It can be inferred that, when TS enhances, less number of hard reinforcement particles catch the part in machining. So, the availability of a large number of hard particles poses a problem of large minor voids leading to rough Ra [12, 31]. The higher TS give less machining action and increases the time of cutting the surface. The AAJM has to penetrate the machining area to improve the cutting area. Finally, interaction plots revealed that at lower conditions of WJP (210 bar), SOD (2 mm) and TS (10 mm/min), the

minimum value of the Ra (2.65 µm) was obtained. The optimum condition of the Ra ($A_1B_1C_1$) was indicated at the lowest levels of input parameters.

3.1.3 Effect of parameters on taper angle (TA)

ANOVA results for TA are observed in Table 7. The agreement of P-value at less than 0.05 levels, i.e., at 95% significance informs that the model is a significant model. The model F-value at 54.45 theorizes a significant fit. F-value upright at 7.52 of 'Lack of Fit' confirms its insignificance. Furthermore, the lack of fit may occur at a 2% probability due to noise. R^2 and Adj. R^2 are mutually comparable at 99.65% and 95.17% respectively. From the table, it can be inferred that the major influencing factors were SOD and WJP.

The empirical model for TA is formulated as Eq. 11.

$$TA = -28.81 + 0.2742 * A - 1.511 * B - 0.1321 * C - 0.000626 * A * A + 0.1962 * B * B + 0.00357 * A * B + 0.000602 * A * C \qquad (11)$$

Table 7 ANOVA for Taper Angle of Al/B$_4$C/Gr composite material

| SS	DF	Seq SS	Adj SS	MS	F-Value	P-Value
Model	7	0.73309	0.73309	0.10472	54.45	0.000
Linear	3	0.59234	0.59234	0.19744	102.66	0.000
A	1	0.39561	0.39561	0.39561	205.68	0.000
B	1	0.18577	0.18577	0.18577	96.59	0.000
C	1	0.01095	0.01095	0.01095	5.70	0.034
2-Way Interaction	2	0.07088	0.07088	0.03544	18.43	0.000
A*B	1	0.00572	0.00572	0.00572	2.98	0.110
A*C	1	0.06516	0.06516	0.06516	33.88	0.000
Error	12	0.02308	0.02308	0.00192		
Lack of fit	7	0.02109	0.02109	0.00301	7.59	0.020
Pure Error	5	0.00198	0.00198	0.00039		
Total	19	0.75617				
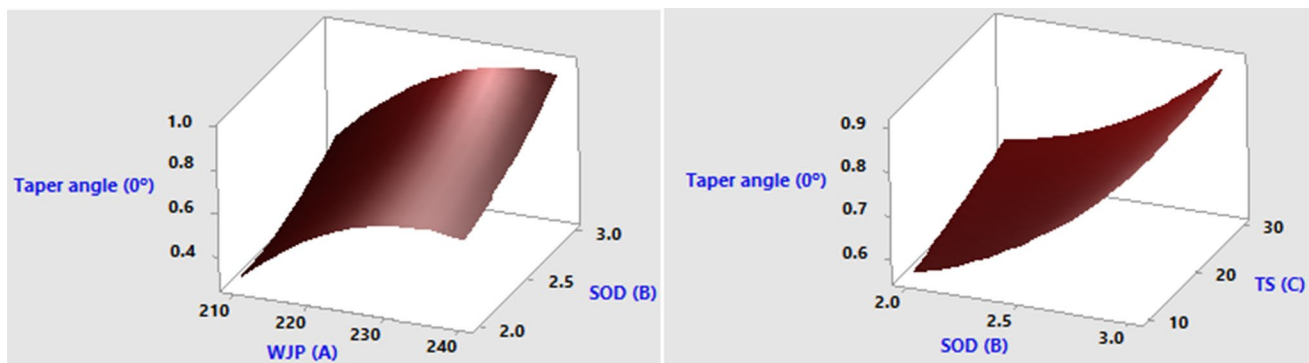
Fig.7 Response plot for Taper Angle (0^0)

The 3D graphs of TA with the efficient interaction input parameters, WJP and TS, WJP and SOD, are shown in Figs. 7a and b respectively. From Fig. 7a, it is understood that TA increases with WJP and TS. As increased WJP produces more kinetic energy of the water jet impinging onto the hybrid composite material, the TA generated will be large. The kinetic energy of the inert abrasive particles increases at maximum hydraulic pressure and enhances the capability for machining [36]. The TA increases with increase in SOD as depicted in Fig. 7b. It is clearly observed that higher SOD tends to achieve a higher TA. The higher SOD allows the water jet to expand together with the normal density of abrasive particles on the outer surface of the divergent AAJ before impinging into the work-piece [31, 32]. Higher and moderate SOD results in minimum divergent and maximum sharpening of the jet, respectively and thus reducing the TA [31]. This explains that TA increases with an increase in TS. However, this leads to a reduction in the cutting ability of the jet due to the damage of the backend abrasive particles. TA is proportional to the kinetic and impact energy of the abrasive mixture and HMMC reinforcement percentage. TA had decreased due to the collisions of the reinforcement particles, this is due to high the hardness of the composite and high energy absorption rate by reinforcement particles in the Al matrix material [37, 38]. This in turn absorbs the impact energy and kinetic energy available in the matrix for machining and reduces taper angle. It was observed that at minimum TA of 0.375 was obtained at the lowest levels of WJP and the medium level and higher levels of SOD and TS. The optimum condition of TA was obtained at 210 bar WJP, 2.5 mm SOD and 30 mm/min TS ($A_1B_2C_3$).

3.2 Multi-objective optimization using TOPSIS approach

For multi-objective optimization, multiple parameters are considered and weights according to their importance are assigned and ranked against each other to find the best solution. This is essentially done by the TOPSIS Approach. The detailed steps of this approach are explained below.

Step1: For this study TA and Ra are considered as lower the better values (non-beneficial attributes), at the same time, MRR is selected as higher the better values (beneficial attributes).

Step 2: To represent in the form of a decision matrix all the experimental data available on the attributes as observed in Table 4.

Step 3: Calculation of the normalized decision matrix is as represented in Table 8.

Table 8 Normalized decision matrix

Expt No	MRR(mm³/min)	Ra (µm)	Taper angle (0°)
1	0.2432	0.2307	0.2834
2	0.1969	0.1885	0.2293
3	0.1985	0.2564	0.2503
4	0.2298	0.1622	0.1185
5	0.2717	0.1781	0.1802
6	0.2181	0.2607	0.2977
7	0.2095	0.2099	0.2184
8	0.2055	0.2075	0.2313
9	0.2542	0.2827	0.3455
10	0.2110	0.2117	0.2214
11	0.2131	0.2130	0.2167
12	0.2071	0.2105	0.2297
13	0.2121	0.2124	0.2307
14	0.2267	0.1983	0.2174
15	0.2389	0.2289	0.0644
16	0.2226	0.2062	0.1245
17	0.2239	0.2405	0.2476
18	0.1689	0.2350	0.1484
19	0.2436	0.2583	0.2662
20	0.2522	0.2417	0.1603

Table 9 Determination of weighted normalized decision

Expt No	MRR(mm³/min)	Ra (µm)	Taper angle (0°)
1	0.0253	0.0675	0.1708
2	0.0204	0.0552	0.1382
3	0.0206	0.0751	0.1508
4	0.0239	0.0475	0.0714
5	0.0282	0.0522	0.1086
6	0.0226	0.0763	0.1794
7	0.0217	0.0615	0.1316
8	0.0213	0.0607	0.1394
9	0.0264	0.0828	0.2082
10	0.0219	0.0621	0.1334
11	0.0221	0.0624	0.1306
12	0.0215	0.0616	0.1384
13	0.0220	0.0622	0.1399
14	0.0235	0.0581	0.1310
15	0.0248	0.0670	0.0387
16	0.0231	0.0604	0.0749
17	0.0232	0.0704	0.1492
18	0.0175	0.0688	0.0894
19	0.0253	0.0756	0.1604
20	0.0262	0.0707	0.0966

Step 4: Weighted normalized decision matrix is calculated as observed in Table 9. The attributed factor weights were selected as TA = 0.6027, Ra = 0.2925 and MRR = 0.103. The weights of attributes sum must be equal to 1.

Step 5: To achieve the best and worst ideal solutions.

$$V_j^+ = \{0.0283, \ 0.0475, \ 0.0388\}$$

$$V_j^- = \{0.0175, \ 0.0827, \ 0.02082\}$$

Step 6: To achieve the separation measures, the calculations are in Table. 10

Step 7: Finding out the relative closeness to the best condition. From the Table the relative closeness coefficient condition is 0.8958, matching to the pilot condition no 15 is observed, at input factor settings of A = 210 bar, B = 2 mm and C = 30 m/min.

Step 8: The assigned TOPSIS ranking scores (C_i) are presented in Table 11.

Then ANOVA is applied for the TOPSIS model and it was observed that important input factors are WJP (55.21%), SOD (23.36%), TS (2.56%), with the interaction of WJP and SOD (6.01%) for AAJM. The effect of major influencing input factors on the multi-objective performance of values, ranks and divisions are mentioned in Table 11. Based on the ANOVA hybrid RSM-TOPSIS results, it was found that WJP plays a significant role in AAJM. Hybrid RSM-TOPSIS response plots and ANOVA values are shown in Fig. 8 and Table 12. $A_1B_1C_3$ settings

Table 11 Relative closeness values and their TOPSIS rankings

Expt No	C_i^+	Rank
1	0.2354	18
2	0.4295	11
3	0.3341	16
4	0.8113	2
5	0.5996	6
6	0.1726	19
7	0.4584	9
8	0.4156	14
9	0.0488	20
10	0.4477	10
11	0.4631	8
12	0.4201	12
13	0.4162	13
14	0.4666	7
15	0.8958	1
16	0.7771	3
17	0.3492	15
18	0.6814	4
19	0.2817	17
20	0.6436	5

of AAJM factors were selected as the optimum levels of factors.

3.3 Confirmation experiments

Table 13 shows the confirmation test results for the best conditions of AAJM input factors to check the enhancement in the output performance measures. From the confirmation test results, it is verified that the residual value is below 5% of the initially conducted RSM-CCD measured values [39, 40]. The hybrid TOPSIS test results indicating that the best input factor setting is $A_1B_1C_3$ has been successfully verified. Table 13 indicates the conformation of the single RSM–CCD results and hybrid RSM-CCD-TOPSIS results of AAJM for hybrid Al 7075/B_4C/ Gr is represented.

4 Conclusion

The present work is carried out to find the best solution of AAJM optimum output measurements of Al 7075/B_4C/Gr with the RSM-TOPSIS method. The result indicated from the present experimental study is extremely helpful for selecting the optimum machining conditions for Al 7075/B_4C/Gr composite, and the following conclusions can be drawn.

1. The optimum MRR was indicated with ($A_1B_3C_1$) optimum condition concerning lower water jet pressure
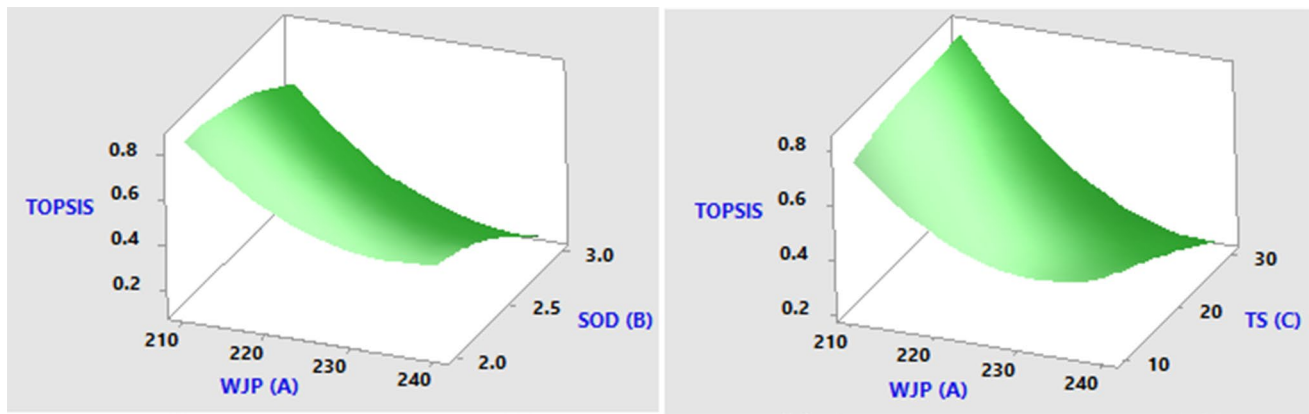
Table 10 Separation measures for positive and negative ideal solutions

Expt No	S^+	S^-
1	0.0253	0.0675
2	0.0204	0.0552
3	0.0206	0.0751
4	0.0239	0.0475
5	0.0282	0.0522
6	0.0226	0.0763
7	0.0217	0.0615
8	0.0213	0.0607
9	0.0264	0.0828
10	0.0219	0.0621
11	0.0221	0.0624
12	0.0215	0.0616
13	0.0220	0.0622
14	0.0235	0.0581
15	0.0248	0.0670
16	0.0231	0.0604
17	0.0232	0.0704
18	0.0175	0.0688
19	0.0253	0.0756
20	0.0262	0.0707

Fig.8 Response plot for RSM-TOPSIS

Table 12 ANOVA for TOPSIS model of Al/B$_4$C/Gr composite material

SS	DF	Seq SS	Adj SS	MS	F-Value	P-Value
Model	8	0.8622	0.8622	0.1077	55.34	0.000
Linear	3	0.7169	0.7169	0.2389	122.71	0.000
A	1	0.4879	0.4879	0.4879	250.53	0.000
B	1	0.2064	0.2064	0.2064	106.00	0.000
C	1	0.0225	0.0225	0.0225	11.60	0.006
2-Way interaction	3	0.0697	0.0697	0.0232	11.93	0.001
A*B	1	0.0096	0.0096	0.0096	4.95	0.048
A*C	1	0.0531	0.0531	0.0531	27.28	0.000
B*C	1	0.0069	0.0069	0.0069	3.56	0.086
Error	11	0.0214	0.0214	0.0019		
Lack of fit	6	0.0189	0.0189	0.0031	6.53	0.020
Pure Error	5	0.0024	0.0024	0.0004		
Total	19	0.8836				

Table 13 Confirmation experimental results

Approach Method	Optimum Condition	Optimal level	MRR (mm^3/ min)	Ra (μm)	Taper Angle (0°)
RSM-CCD	Single		A$_1$B$_3$C$_1$	A$_1$B$_1$C$_1$	A$_1$B$_2$C$_3$
			5.3118	2.65	0.375
RSM-CCD-TOPSIS	Multi	A$_1$B$_1$C$_3$	4.8703	3.57	0.189

(210 bar), higher Stand-off distance (3 mm), and lower traversing speed (10 mm/min). The occurred maximum MRR value is at 5.311 mm^3/min and corresponding values of R^2 value and Adj. R^2 are 98.83% and 98.29% respectively.

2. The desirable lower Ra was obtained at 2.65 μm and conditions were (A$_1$B$_1$C$_1$); 210 bar jet pressure, 2 mm Stand-off distance and 10 mm/min traversing speed and correlating values of R^2 value and Adj. R^2 are 99.07% and 98.65% respectively.

3. The optimum value for taper angle was 0.375°, and dominating input factors are set at (A$_1$B$_2$C$_3$): lower jet pressure (210 bar), Stand-off distance (2.5 mm), and higher traverse speed (30 mm/min), corresponding values of R^2 value and Adj. R^2 are 99.65% and 95.17% respectively.

4. The corresponding value recommended through the RSM-TOPSIS method indicated that optimum lower input factors were jet pressure and Stand-off distance and higher factors were traversing speed, it will give the best experimental setting for experimental condi-

tion 15 and corresponding values of R^2 value and Adj. are 99.91% and 95.81% respectively.

5. The RSM-TOPSIS test results indicated that the best input factor setting is $A_1B_1C_3$ and from ANOVA results, it is observed that distributing important input factors are jet pressure (55.21%), Stand-off distance (23.36%), and traverse speed (2.56%).

6. From the Hybrid RSM-TOPSIS approach results was observed that the TA was 49.6% less than the value predicted by the RSM-CCD approach. These AAJ machining results will be beneficial for applications in the automobile, aerospace, and structural engineering sectors.

Declarations

References

1. Razavi M, Rajabi-Zamani AH, Rahimipour MR, Kaboli R, Shabani MO, Yazdani Red R (2011) Synthesis of Fe-TiC-Al_2O_3 hybrid nano composite via carbothermal reduction enhanced by mechanical activation. Ceram Int 37(2):443–449

2. Velickovicl S, Stojanovicl B, Babicl M, Vencl A, Bobic I, Bognar GV, Vucetic F (2019) Parametric optimization of the aluminium nanocomposites wear rate. J Braz Soc Mech Sci Eng 41(1):19

3. Mazahery A, Shabani MO (2012) Tribological behavior of semi-solid- semisolid compocast Al-Si matrix composites reinforced with TiB_2 coated B_4C particulates. Ceram Int 38(3):1887–1895

4. Prof. Kainer KU (2006) Metal Matrix Composites: Custom-made Materials for Automotive and Aerospace Engineering, ISBN: 9783527608119

5. Shihab SK, Gattmah J, Kadhim HM (2020) Experimental investigation of surface integrity and multi-objective optimization of end milling for hybrid Al 7075 matrix composites. SILICON. https://doi.org/10.1007/s12633-020-00530-1

6. Malhotra P, Singh NK, Tyagi RK, Sikarwar BS (2020) Comparative study of rotary-EDM, gas assisted-EDM, and gas assisted powder mixed-EDM of the hybrid metal matrix composite. Adv Mater Process Technol. https://doi.org/10.1080/2374068X.2020.1855398

7. Ponappa K, Sasikumar KSK, Sambathkumar M, Udhayakumar M (2019) Multi objective optimization of EDM process parameters for machining of hybrid aluminum metal matrix composites(Al7075/Tic/B4C)using genetic algorithm. Surf Rev Lett 26(10):1950071

8. Thamizhvalavan P, Arivazhagan S, Yuvaraj N, Ramesh B (2019) Machinability study of abrasive aqua jet parameters on hybrid metal matrix composite. Mater Manuf Process 34(3):321–344

9. Manoj M, Jinu GR, Muthuramalingam T (2018) Multi response optimization of AWJM process parameters on machining TiB_2 particles reinforced Al7075 composite using Taguchi-DEAR methodology. SILICON 10(5):2287–2293

10. Dhanawade A, Kumar P, Kumar S (2020) Experimental study on abrasive water jet machining of carbon epoxy composite. Adv Mater Process Technol 6(1):40–53

11. Siddiqui TU, Shukla M (2008) Experimental investigation and hybrid multi-response robust parameter design in abrasive water jet machining of aircraft grade layered composites. IJAEA 1(5):39–48

12. Sasikumar KSK, Arulshri KP, Ponappa K, Uthayakumar M (2018) A study on kerf characteristics of hybrid aluminium 7075 metal matrix composites machined using abrasive water jet machining technology. Proc Inst Mech Eng Part B J Eng Manuf 232(4):690–704

13. Kumar D, Gururaja S (2020) Abrasive waterjet machining of Ti/CFRP/Ti laminate and multi-objective optimization of the process parameters using response surface methodology. J Compos Mater 54(13):1741–1759

14. Iqbal A, Dar NU, Hussain G (2011) Optimization of abrasive water jet cutting of ductile materials. J Wuhan Univ Technol Mater Sci Ed 26(1):88–92

15. Kumar A, Singh H, Kumar V (2018) Study the parametric effect of abrasive water jet machining on surface roughness of Inconel 718 using RSM-BBD techniques. Mater Manuf Process 33(13):1483–1490

16. Kumar KR, Sreebalaji VS, Pridhar T (2018) Characterization and optimization of abrasive water jet machining parameters of aluminium/tungsten carbide composites. Measurement 117:57–66

17. Tofigh AA, Rahimipour MR, Shabani MO, Davami P (2015) Application of the combined neuro-computing, fuzzy logic and swarm intelligence for optimization of compocast nanocomposites. J Compos Mater 49(13):1653–1663

18. Tofigh AA, Shabani MO (2013) Efficient optimum solution for high strength Al alloys matrix composites. Ceram Int 39(7):7483–7490

19. Shabani MO, Shamsipour M, Mazahery A, Pahlevani Z (2018) Performance of ANFIS coupled with PSO in manufacturing superior wear resistant aluminum matrix nano composites. Trans Indian Inst Met 71(9):2095–2103

20. Akbari M, Shojaeefard MH, Asadi P, Khalkhali A (2017) Hybrid multi-objective optimization of microstructural and mechanical properties of B4C/A356 composites fabricated by FSP using TOPSIS and modified NSGA-II. Trans Nonferrous Metals Soc China 27(11):2317–2333

21. Shabani MO, Rahimipour MR, Tofigh AA, Davami P (2015) Refined microstructure of compo cast nanocomposites: the performance of combined neuro-computing, fuzzy logic and particle swarm techniques. Neural Comput Appl 26(4):899–909

22. Shamsipour M, Pahlevani Z, Shabani MO, Mazahery A (2017) Squeeze casting of electromagnetically stirred aluminum matrix nanocomposites in semi-solid condition using hybrid algorithm optimized parameters. Kovove Mater 55(1):33–43

23. Myers RH, Montgomery DC, Anderson-Cook CM (2016) Response surface methodology: process and product optimization using designed experiments. Wiley

24. Deshpande YV, Andhare AB, Padole PM (2018) Experimental results on the performance of cryogenic treatment of tool and minimum quantity lubrication for machinability improvement in the turning of Inconel 718. J Braz Soc Mech Sci Eng 40(1):6

25. John MS, Balaji B, Vinayagam BK (2017) Optimisation of internal roller burnishing process in CNC machining center using response surface methodology. J Braz Soc Mech Sci Eng 39(10):4045–4057

26. Opricovic S, Tzeng GH (2004) Compromise solution by MCDM methods: A comparative analysis of VIKOR and TOPSIS. Eur J Oper Res 156(2):445–455

27. Dr. Gupta G, Prof. Gupta MK, Springer series in advanced manufacturing, Springer International Publishing, ISBN: 978-3-030-19637-0

28. Saaty TL (1980) The analytic hierarchy process. McGraw-Hill, New York

29. Tripathy S, Tripathy DK (2017) Multi-response optimization of machining process parameters for powder mixed electro-discharge machining of H-11 die steel using grey relational analysis and topsis. Mach Sci Technol 21(3):362–384

30. Ram Prasad AVS, Ramji K, Kolli M, Vamsi Krishna G (2019) Multi-response optimization of machining process parameters for wire electrical discharge machining of lead-induced ti-6al-4v alloy using AHP–TOPSIS method. J Adv Manuf Syst 18(2):213–236

31. Raj RR, Kanagasabapathy H (2018) Influence of abrasive water jet machining parameter on performance characteristics of AA7075-ZrSiO4-hBN hybrid metal matrix composites. Mater Res Express 5(10):106509

32. Gnanavelbabu A, Rajkumar K, Saravanan P (2018) Investigation on the cutting quality characteristics of abrasive water jet machining of AA6061-B4C-hBN hybrid metal matrix composites. Mater Manuf Process 33(12):1313–1323

33. Mm IW, Azmi AI, Lee CC, Mansor AF (2018) Kerf taper and delamination damage minimization of FRP hybrid composites under abrasive water-jet machining. Int J Adv Manuf Technol 94(5–8):1727–1744

34. Momber AW, Kovacevic R (2012) Principles of abrasive water jet machining. Springer Science & Business Media

35. Kechagias J, Petropoulos G, Vaxevanidis N (2012) Application of Taguchi design for quality characterization of abrasive water jet machining of TRIP sheet steels. Int J Adv Manuf Technol 62(5–8):635–643

36. Mardi KB, Dixit AR, Srivastava AK, Mallick A, Scucka J, Hlaváček P, Hloch S, Zeleňák M (2018) Effect of water pressure during abrasive waterjet machining of Mg-based nanocomposite. Applications of Fluid Dynamics. Springer, Singapore, pp 605–612

37. Parikh PJ, Lam SS (2009) Parameter estimation for abrasive water jet machining process using neural networks. Int J Adv Manuf Technol 40(5–6):497–502

38. Gnanavelbabu A, Saravanan P, Rajkumar K, Karthikeyan S, Baskaran R (2018) Effect of abrasive waterjet machining parameters on hybrid AA6061-B4C-CNT composites. Mater Today Proceed 5(5):13438–13450

39. Kuo Y, Yang T, Huang GW (2008) The use of a grey-based Taguchi method for optimizing multi-response simulation problems. Eng Optim 40(6):517–528

40. Yang T, Chou P (2005) Solving a multiresponse simulation-optimization problem with discrete variables using a multiple-attribute decision-making method. Math Comput Simul 68(1):9–21